JPE 9-6-6

Battery Energy Storage Based Voltage and Frequency Controller for Isolated Pico Hydro Systems

Bhim Singh* and V. Rajagopal†

†*Dept. of Electrical Engineering, Indian Institute of Technology, Delhi, India

ABSTRACT

This paper deals with an integrated voltage and frequency (VF) controller for isolated asynchronous generators (IAG) driven by a constant power pico-hydro uncontrolled turbine feeding three-phase four-wire loads. The proposed VF controller is used to control the frequency and voltage of an IAG with load leveling. Such a VF controller is also known as an integrated electronic load controller (IELC) which is realized using an isolated star/polygon transformer with a voltage source converter (VSC) and a battery at its DC bus. The proposed generating system with a VFC is modeled and simulated in MATLAB along with Simulink and Simpower system (SPS) toolboxes. The simulated results are presented to demonstrate the performance of an isolated asynchronous generator feeding three-phase four-wire loads with neutral current compensation.

Keywords: Battery energy storage system, Isolated asynchronous generator, Voltage and frequency controller, Integrated electronic load controller

1. Introduction

With the increasing demand for energy and the soaring prices of fossil fuels, it is becoming difficult to reach consumers in remote and isolated places. This leads to the development of small isolated generating plants. Such generating plants may be realized using an asynchronous generator with a capacitor bank to meet the reactive power requirement [1]. Asynchronous generators are robust and brushless, thus they are reduced in size and require less maintenance when compared with synchronous generators. Isolated asynchronous generators (IAG) have emerged as a prime contender for isolated power generation using uncontrolled pico-hydro turbines [2-4]. Although IAGs have many advantages they also have the problems of poor voltage and frequency profiles. A substantial amount of research has been done on frequency and voltage controllers for constant speed applications for feeding three-phase four-wire loads or single phase loads. Most of the electronic load controllers (ELCs) control the frequency and voltage by dissipating the excess energy into an auxiliary load when the load requirement of consumers is less than the generator power [5-8]. All these controllers overlook the power quality issues and the excess power is dissipated in an auxiliary load [9].

In this paper an attempt is made on an integrated electronic load controller (IELC) with a battery on its DC bus working as a VFC [10]. This type of IELC configuration controls voltage and frequency and improves power quality problems. This integrated electronic load controller along with a battery ensures bidirectional power flow from the IAG to the battery under reduced loading periods and from the battery to the

Manuscript received May 30, 2009; revised Sept. 18, 2009
†Corresponding Author: rajsarang@gmail.com
Tel: +91-011-2659-1045, Fax: +91-011-2658-1606, IIT
*Dept. of Electrical Engineering, Indian Institute of Technology, Delhi, India

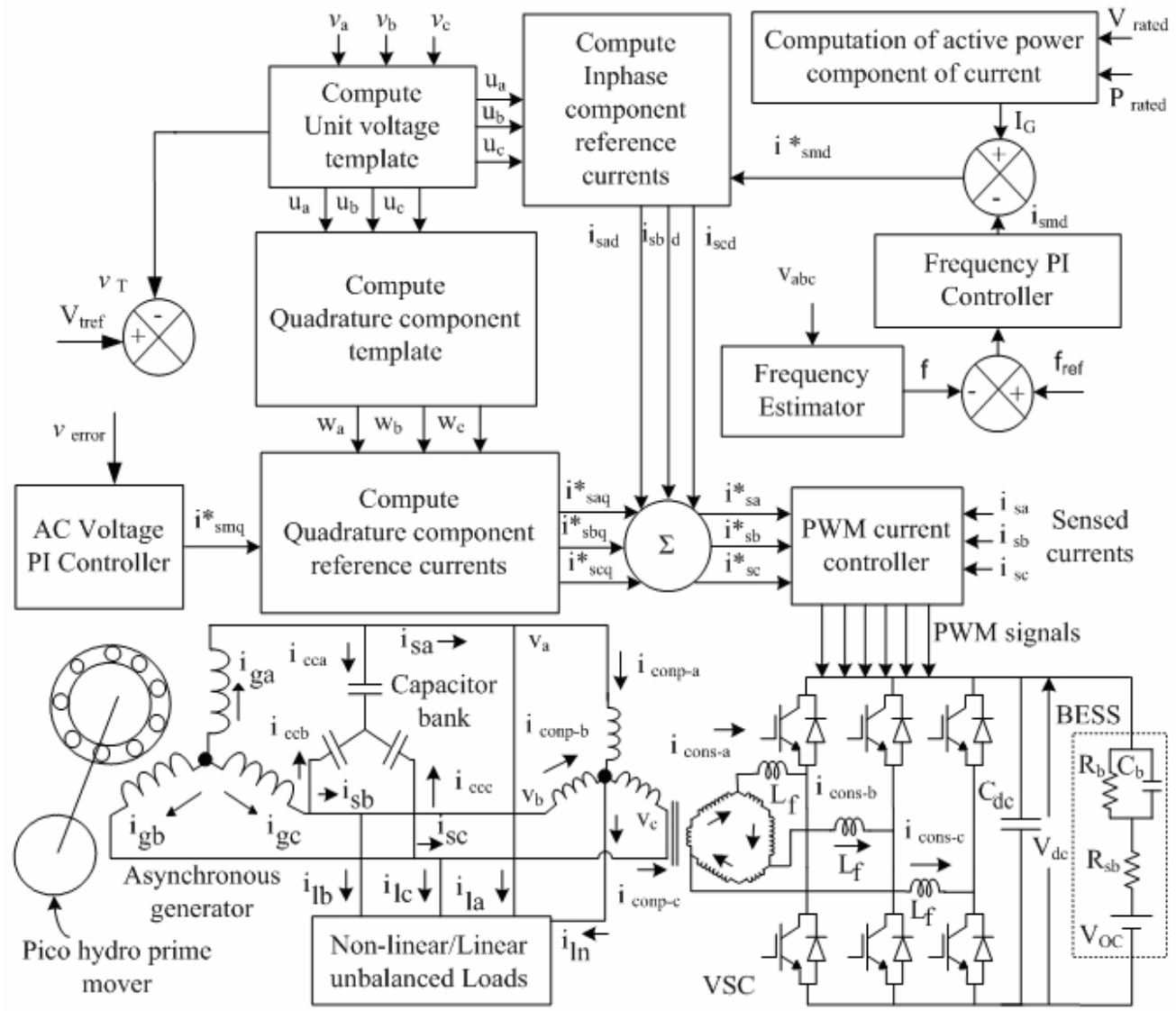

Fig.1. Schematic diagram of IAG with VF controller and its control scheme.

load under peak load periods. The proposed voltage and frequency controller is capable of harmonic elimination, load balancing, neutral current compensation and feeding to the load under peak load conditions [11-13].

2. System Configuration and Principle of Operation

Fig. 1 shows the schematic diagram of the proposed IAG system along with a VF controller, an excitation capacitor, consumer loads and its control algorithm. The proposed VF controller consists of a battery at the DC bus of a VSC (voltage source converter). The battery absorbs the excess active power which is not consumed by consumer loads [10]. A star/polygon transformer is used for isolation, to provide a neutral terminal for 4-wire loads and optimized DC bus voltage at the required level [14]. The value of a star connected excitation capacitor bank is selected to generate the rated voltage at no load while the additional demand of reactive power for the generator and the loads is met by the VF controller. The basic principle of regulating the voltage is reactive power control of the VSC of a VF controller. The active power is controlled by

the battery on the DC bus of the VSC.

Fig. 1 also shows a control scheme for the proposed voltage and frequency controller to regulate the frequency and voltage of the IAG. The control scheme is based on the deviation of reference source currents (which have two components in-phase and quadrature with AC voltage). The in-phase amplitude templates (u_a, u_b and u_c) are derived by dividing the three phase voltages v_a, v_b and v_c by their amplitude V_t. Another set of quadrature unity amplitude templates (w_a, w_b and w_c) is derived from the in-phase unit templates (u_a ,u_b and u_c).

To regulate the AC terminal voltage, its amplitude (V_t) is compared with the reference terminal voltage (V_{tref}). The voltage error is given to the PI (proportional-integral) controller. The output of the PI controller (I_{smq}^*) for the AC voltage control loop decides the amplitude of the reactive current to be generated by the VFC. Multiplication of the quadrature unit vectors (w_a, w_b and w_c) with the output of the PI based AC voltage controller (I_{smq}^*) yields the quadrature component of the reference source currents (i_{saq}*, i_{sbq}* and i_{scq}*). Moreover, the function of frequency control using the battery energy storage system (BESS) decides the active power flow. The BESS absorbs the excess active power when the system frequency is above the reference value and it delivers active power when system frequency is less than the reference value or there is a deficiency in the generated power which results in an inability to meet the demand of consumer loads. For generating the active components of the reference source currents, the output of the frequency PI controller (I_{msd}) is compared with the rated generator current (I_G) and the difference between these two currents is considered as an amplitude of the in-phase component of the reference source current (I_{msd}*). Multiplication of the in-phase unit vectors (u_a, u_b and u_c) with the output of the PI controller (I_{smd}^*) yields the in-phase component of the reference source currents (i_{sad}*, i_{sbd}*and i_{scd}*). The sum of the quadrature and the in-phase components are the reference source currents (i_{sa}*, i_{sb}* and i_{sc}*), which are compared with the sensed source currents (i_{sa}, i_{sb} and i_{sc}). These current error signals are amplified and compared with the triangular carrier wave to generate gating signals for the IGBTs (insulated gate bipolar transistor) of the VSC of a VFC.

3. Design of the Proposed IAG System

The proposed IAG system consists of an asynchronous generator, a capacitor bank, a star/polygon transformer, interfacing inductors, a voltage source converter, a DC bus capacitor, a battery etc. The design and selection of these components are given in this section.

3.1 Design of the Electrical System

The electrical system consists of a 7.5 kW, 415 V, 50 Hz, Y connected, 4-Pole squirrel cage asynchronous machine with an excitation capacitor. A star connected capacitor bank is installed to generate the rated voltage at no load. To get the rated voltage at no load at the IAG terminals, a 4.6 kVAR capacitor bank is used [9].

3.2 Design of the Star/Polygon Transformer

The three phase supply voltage applied to the input of the transformer [14] shown in Fig. 2 is as follows:

$$V_a = V\angle 0°;\ V_b = V\angle 120°;\ V_c = V\angle -120° \quad (1)$$

$$V_{ab} = \sqrt{3}V\angle -30°;\ V_b = \sqrt{3}V\angle 90°;\ V_c = \sqrt{3}\,V\angle -150° \quad (2)$$

If the transformation ratio is 'a' = V_{ab}/V_{AB}, then the secondary winding line voltage is given as:

$$V_{AB} = (K_1 V_{ab} - K_2 V_{bc})/a \quad (3)$$

$$V_{BC} = (K_1 V_{bc} - K_2 V_{ca})/a \quad (4)$$

$$V_{CA} = (K_1 V_{ca} - K_2 V_{ab})/a \quad (5)$$

The values of the constants K_1 and K_2 determine the winding turns as a fraction of the input phase voltage and these are obtained as K_1=0.8453, K_2=0. 3094 and a=3.77. In Fig 2, these voltages are as follows:

$V_a = V_b = V_c = 415/\sqrt{3} = 239.6$V

$V_{a23a24} = 89.83$V, $V_{a21a22} = 32.88$V

Therefore a set of three transformers of voltage rating 239.6 V/89.83V/32.88 V is selected to form the required star/polygon transformer.

The rating of this transformer is dependent on the voltage across each winding and the current through it. The winding voltages determine the core size while the currents determine the conductor size and hence the two

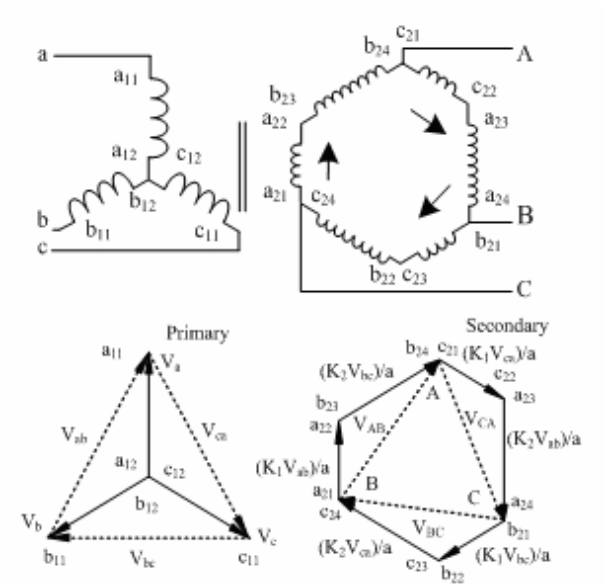

Fig. 2. Star / polygon transformer and its phasor diagram.

determine its VA rating. The VA rating of these transformers is calculated as: VA rating =0.5Σ (V_k I_k), where V_k and I_k are the root mean square (rms) values of voltage across and current through the k^{th} winding [14]. Hence, three single-phase transformers of rating 2.51 kVA, 239.6 V/89.83V/32.88 V are used to form the required star/polygon transformer.

3.3 DC Capacitor Voltage

The minimum dc bus voltage of the VSC of a VF controller should be greater than twice the peak of the phase voltage of the IAG system. The dc bus voltage is calculated as:

$$V_{dc} = (2\sqrt{2}\, V_{LL})/(\sqrt{3}\, m) \quad (6)$$

where m is the modulation index and it is considered as 1 and V_{LL} is the secondary line voltage of the VF controller. Thus V_{dc} is obtained as 180.4 V for the V_{LL} of 110 V and it is selected as 192V to be an integer multiple of 12 V battery cells.

3.4 Design of the AC Inductor

The selection of ac inductance (L_f) of the VSC of a VF controller depends on current ripple $i_{cr(p\text{-}p)}$, switching frequency f_s, dc bus voltage (V_{dc}) and L_f is given [15] as:

$$L_f = (\sqrt{3} m V_{dc})/(12 a_L f_s i_{cr(p-p)}) \quad (7)$$

where m is the modulation index and 'a_L' is the overloading factor and when considering that $i_{cr(p\text{-}p)} = 5\%$, f_s =10 kHz, m=1, V_{dc} = 192 V, a = 1.2 and the L_f is 4.4mH. A round-off value of L_f of 4.5mH is selected in this investigation.

3.5 Design of the DC Bus Capacitor

The value of the dc capacitor (C_{dc}) of the VSC of a VF controller depends on instantaneous energy being available to the VSC during transients. The principle of energy conservation is applied as [15]:

$$\frac{1}{2} C_{dc} [(V_{dc}^2) - (V_{dc1}^2)] = 3 V_{ph} (a_L I)\, t \quad (8)$$

where V_{dc} is the reference dc voltage, V_{dc1} is the minimum voltage of the dc bus, a_L is the overloading factor, V_{ph} is the phase voltage, I is the phase current and 't' is the time by which the dc bus voltage is to be recovered.

Considering the minimum voltage level of the dc bus, V_{dc1} = 186 V, V_{dc} = 192 V, V_{ph} = 110V, I = 14.5 A, t= 350 μs and a_L= 1.2, the calculated value of C_{dc} is 2777 μ F and it is selected as 3000μF.

3.6 Design of the VF Controller

The VSC voltage rating (V_{sw}) of the solid state device (IGBT) can be calculated under the dynamic condition as:

$$V_{sw} = (V_{dc} + V_d) \quad (9)$$

where V_d is a 10% overshoot in the dc link voltage under extreme conditions.

Therefore, using eqn. (9) the switch voltage rating is as:

V_{sw} = 192 + 10% of 192 = 211.2 V.

The rated current, which flows through the three leg VSC is 'I' (the secondary line current of the star/polygon transformer). The peak value of the current is √2 I, where 'I' is the required current flow through the VSC considering a safety factor of 1.25. The maximum device current can be calculated as:

$$I_{sw} = 1.25\ (i_{Lripple(p\text{-}p)} + I_{s\ (peak)}) \quad (10)$$

= 1.25 (5% of peak value rated current + peak value of rated current) = 107.65 A

Therefore a solid state switch (IGBT) of 450 V and 150 A is selected to form the VSC of a VFC.

3.7 Design of the Battery Rating

Here a battery is considered to have 7.5 kW for 6-hours of peak capacity and 16 batteries in each row of 12 V each. The variation in its voltage from 186 V to 206 V is considered for discharged and charged conditions.

The equivalent capacitor (C_b) in the Thevenin equivalent circuit of the battery shown in Fig. 1 is used to model the battery unit. The capacitance (C_b) can be determined from:

$$C_b = \frac{kWh\ X\ 3600\ X\ 10^3}{0.5\,(V_{oc\,max}^2 - V_{oc\,min}^2)} = 41326F \quad (11)$$

where V_{ocmax} and V_{ocmin} are the minimum and maximum open circuit voltages of the battery under the fully charged and discharged conditions.

In the Thevenin's equivalent model of the battery, R_s is equivalent to the resistance of the parallel and series combination of batteries consisting of cells of 12V, which is usually a small value. The parallel circuit of R_b and C_b is used to describe the stored energy and voltage during the charging or discharging of the battery. R_b in parallel with C_b represents the self discharging of the battery. The discharging current of the battery is quite small so the value of resistance is considered in kilo ohms.

4. Control Algorithm

Fig. 1 shows the control scheme of an IAG system. The basic equations of this control scheme for voltage and frequency control are given as follows.

4.1 In-Phase Component of the Reference Source Currents

The in-phase component of the reference source currents is estimated by taking the difference in the amplitude of the rated generated current (I_G) and the output of the frequency PI controller (I_{smd}). The frequency error is defined as:

$$f_{er}(n) = f_{ref(n)} - f_{(n)} \quad (12)$$

where f_{ref} is the reference frequency (50 Hz in the present system) and "f" is the frequency of the voltage of an IAG. The instantaneous value of "f" is estimated using the phase locked loop (PLL) over the ac terminal voltages (v_a, v_b and v_c).

At the n^{th} sampling instant, the output of the frequency PI controller (I_{smd}) is as:

$$I_{smd(n)} = I_{smd(n-1)} + K_{pf}\{f_{re(n)} - f_{re(n-1)}\} + K_{if}\, f_{re(n)} \quad (13)$$

where K_{pf} and K_{if} are the proportional and integral gains of the frequency PI controller.

By eqn. (12) and eqn. (13) at the nth sampling instant, the amplitude of the active component of the source currents is as:

$$I_{smd} = I_{G(n)} - I_{smd(n)} \quad (14)$$

The three-phase voltages at the IAG terminals (v_a, v_b and v_c) are considered to be sinusoidal and hence their amplitude is computed as:

$$V_t = \{(2/3)\,(v_a^2 + v_b^2 + v_c^2)\}^{1/2} \quad (15)$$

The unit vectors in phase with v_a, v_b and v_c are derived as:

$$u_a = v_a/V_t;\ u_b = v_b/V_t;\ u_c = v_c/V_t \quad (16)$$

The in-phase components of the reference source currents are estimated as:

$$i^*_{sad} = I^*_{smd}\, u_a;\ i^*_{sbd} = I^*_{smd}\, u_b;\quad i^*_{scd} = I_{smd}\, u_c \quad (17)$$

4.2 Quadrature Component of the Reference Source Currents

The voltage error V_{er} is the amplitude of the AC voltage at the n^{th} sampling instant as in:

$$V_{er(n)} = V_{tref(n)} - V_{t(n)} \quad (18)$$

where $V_{tref(n)}$ is the amplitude of the reference AC terminal voltage and $V_{t(n)}$ is the amplitude of the sensed three-phase AC voltages at the IAG terminals at the n^{th} instant.

The output of the PI controller ($I^*_{smq(n)}$) for maintaining the amplitude of the AC terminal voltage at a constant value at the n^{th} sampling instant is expressed as:

$$I^*_{smq(n)} = I^*_{smq(n-1)} + K_{pa} \{ V_{er(n)} - V_{er(n-1)} \} + K_{ia} V_{er(n)} \quad (19)$$

where K_{pa} and K_{ia} are the proportional and integral gain constants of the proportional integral (PI) controller, $V_{er(n)}$ and $V_{er(n-1)}$ are the voltage errors in the n^{th} and $(n-1)^{th}$ instants and $I^*_{smq(n-1)}$ is the amplitude of the quadrature component of the reference source current at the $(n-1)^{th}$ instant.

The quadrature components of the reference source currents are estimated as:

$$i^*_{saq} = I^*_{smq} w_a; \quad i^*_{sbq} = I^*_{smq} w_b; \quad i^*_{scq} = I^*_{smq} w_c \quad (20)$$

These unit vectors (w_a, w_b and w_c) in quadrature with v_a, v_b and v_c may be derived using a quadrature transformation of the in-phase unit vectors u_a, u_b and u_c as:

$$w_a = -u_b / \sqrt{3} + u_c / \sqrt{3} \quad (21)$$

$$w_b = \sqrt{3}\, u_a / 2 + (u_b - u_c) / 2\sqrt{3} \quad (22)$$

$$w_c = -\sqrt{3}\, u_a / 2 + (u_b - u_c) / 2\sqrt{3} \quad (23)$$

4.3 Total Reference Source Currents

The total reference source currents are the sum of the in-phase and the quadrature components of the reference source currents as:

$$i^*_{sa} = i^*_{saq} + i^*_{sad} \quad (24)$$

$$i^*_{sb} = i^*_{sbq} + i^*_{sbd} \quad (25)$$

$$i^*_{sc} = i^*_{scq} + i^*_{scd} \quad (26)$$

These reference source currents are fed to the PWM current controller of the VSC of a VF controller.

4.4 PWM Signal Generator

The reference source currents (i^*_{sa}, i^*_{sb} and i^*_{sc}) are compared with the sensed source currents (i_{sa}, i_{sb} and i_{sc}) in the PWM current controller. The current errors for all the phases are amplified and the amplified current errors are compared with a fixed frequency triangular carrier wave (10kHz in this case) to generate the gating signals of the IGBTs of the VSC of a VF controller.

5. Modeling of the IAG System

A model of the battery energy storage system based VF controller for an IAG driven by a pico hydro turbine, the linear and non linear loads, the interfacing inductors and excitation capacitor bank, the star/polygon transformer, the control scheme and a battery, are developed in MATLAB. The modeling of an IAG is carried out using a 7.5 kW, 415 V, 50 Hz, Y-connected 4-pole asynchronous machine and a 4.6 kVAR Y-connected excitation capacitor bank. The saturation characteristics of the machine is considered by performing a synchronous speed test and the data given in the appendices is used in the model of the machine in the Simpower system (SPS) tool box of MATLAB version 7.5. The VF controller is realized as a three–leg VSC with a battery at the DC bus. Both the linear and the non linear loads are considered to demonstrate the capability of the VF controller. The simulation is carried out in discrete mode at 10e-6 step size with an ode23tb solver.

6. Results and Discussion

The performance of the proposed VF controller is studied for an uncontrolled pico-hydro turbine with a constant power input driven isolated asynchronous generator feeding linear/nonlinear balanced/unbalanced three-phase four-wire loads. Fig 3 shows its performance with unbalanced linear loads and Figs 4, and 5 show its performance with unbalanced nonlinear loads. Figs 3 and 4 show the waveforms of the IAG terminal voltages (v_{abc}), the source currents (i_{sabc}), the capacitor bank current (i_{cca}), the load currents (i_{La}, i_{Lb} and i_{Lc}), the VFC currents on primary and secondary side of a star/polygon transformer (i_{conp}, i_{cons}), the load neutral current (i_{ln}), the battery current (i_b), the IAG terminal voltage (V_t) and its reference amplitude, the DC bus voltage (Battery voltage) (v_{dcref}, v_{dc}), the IAG speed (ω), the frequency (f) and the powers

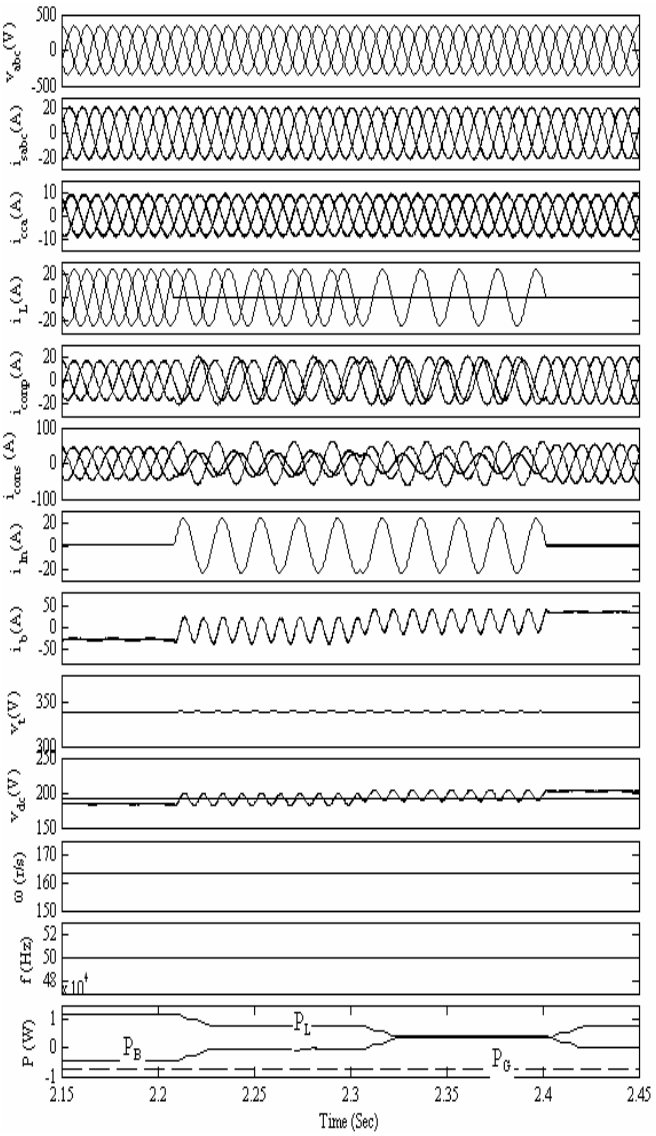

Fig. 3. Performance of IAG with VFC feeding a three – phase four wire linear loads.

for the source (P_G), battery (P_B) and load (P_L) during different dynamic load conditions.

6.1 Performance of the IAG with a VF Controller with Balanced/Unbalanced Linear Loads

Fig. 3 shows the performance of the VF controller under the application of balanced/unbalanced linear loads on an IAG system driven by a constant power pico hydro turbine. All three single phase loads are fed by an IAG of 3.5 kW each. The battery supplies the deficit amount of power to the load. At 2.2 sec one phase load is removed

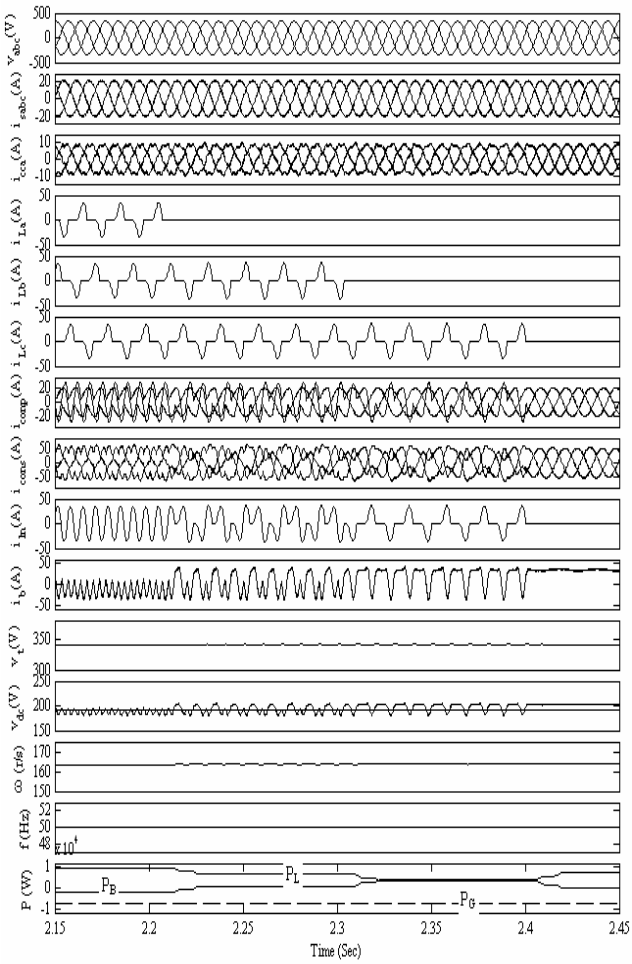

Fig. 4. Performance of IAG with feeding a three – phase four wire non linear loads.

and the IAG starts charging the battery with the excess amount of power. At 2.3 sec the second phase load is removed and the IAG charges the battery with the extra power. At 2.4 sec all three phase loads are removed and the IAG feeds all the power to the battery. The transformer exhibits unbalanced currents and it provides neutral current compensation of the load.

6.2 Performance of the IAG with a VF Controller with Balanced/Unbalanced Non Linear Loads

Fig. 4 shows the performance of the VF controller under the application of balanced/unbalanced nonlinear loads on an IAG system driven by a constant power pico hydroturbine. At 2.15 sec all three single phase loads are

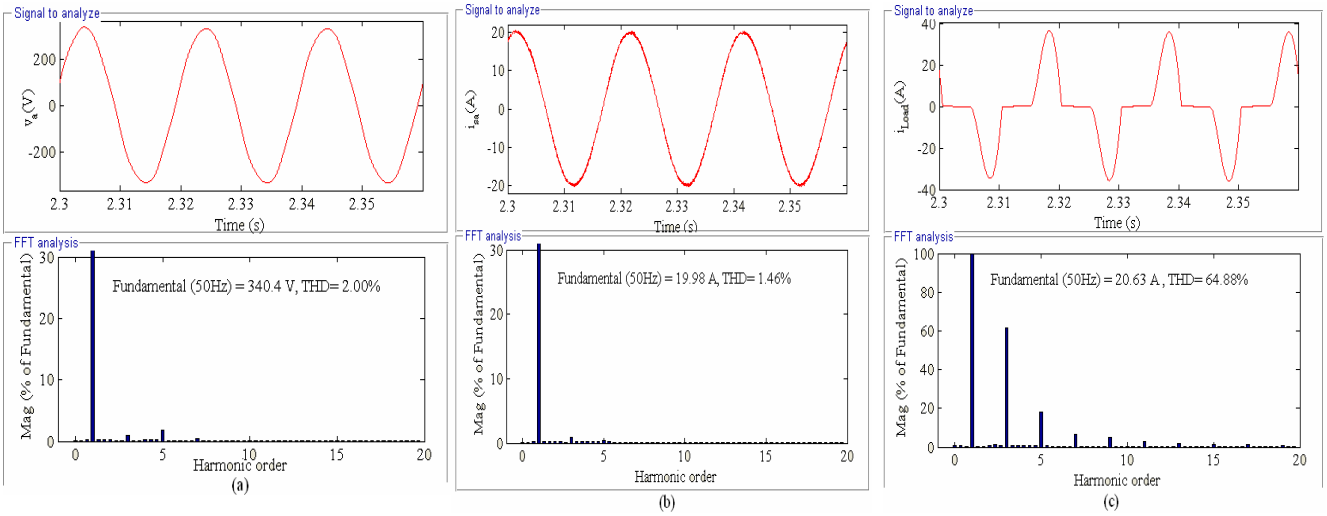

Fig. 5. Harmonic spectra of (a) source voltage (v_a), (b) source current (i_{sa}) and (c) load current (i_{Load}) under balanced nonlinear condition.

fed by an IAG of 2.75 kW each. The battery supplies the deficit amount of power to the load. At 2.2 sec one phase load is removed and the IAG charges the battery with the slightly higher excess amount of power. At 2.3 sec the second phase load is removed and the IAG charges the battery with excess power. At 2.4 sec the total three phase load is removed and the IAG supplies the total generated power to the battery. The transformer has the unbalanced currents providing load current compensation. Fig 5 (a) shows the source voltage waveform and its harmonic spectrum, which has a THD (Total Harmonic Distortion) of 2.0%, Fig 5 (b) shows the source current waveform and its harmonic spectrum which has a THD of 1.46%, Fig 5 (c) shows the nonlinear load current waveform and its harmonic spectrum which has a THD of 64.88%. The THD of the terminal voltage of the generator is well within the 5% limit imposed by the IEEE-519 standard. In this way, it is demonstrated that the proposed VF controller also provides the function of a harmonic eliminator [10].

7. Conclusions

A simple standalone uncontrolled pico-hydro turbine driven asynchronous generator system with a VF controller has been designed and modeled. Its performance has been simulated and demonstrated under different loading conditions (balanced/unbalanced linear/nonlinear). It has been observed that the VF controller produces satisfactory performance under different loading conditions along with frequency and voltage control, load balancing, neutral current compensation and harmonic elimination.

Appendices

A. Parameters of 7.5 kW, 415 V, 50 Hz, Y connected, 4 - Pole Asynchronous Machine

R_s=1 Ω, R_r= 0.77 Ω, X_{lr}=X_{ls}=1.5Ω, J=0.1384 kg – m^2

L_m = 0.134 H (I_m< 3.16)

$L_m = 9e^{-5} I_m^2 - 0.0087 I_m + 0.1643$ (3.16<I_m<12.72)

L_m = 0.068 H (I_m> 12.72)

B. Controller parameters

L_f = 4.5mH; R_f = 0.1Ω and C_{dc}= 3000 μF,

AC voltage PI controller: K_{pa} =0.02, K_{ia} = 0.02.

Frequency PI controller K_{pd} = 0.01, K_{id} =0.01

C. Prime mover Characteristics

$T_{shaft} = (K_1 - K_2\ \omega_m)$; K_1= 1465, K_2 = 8.8

D. Battery specification

R_b = 0.1 Ω, R_{sb} = 5 kΩ, C_b = 41326F; V_{oc} = 192V.

References

[1] Y. Zidani, M. Naciri, "A numerical analytical approach for the optimal capacitor used for the self excited induction generator," *Proceedings of IEEE Power Electronics*

Specialists Conf. (PESC' 2001), Vol. 1, pp. 216~220, Jun. 2001.

[2] J. M. Elder, J. T. Boys and J. L. Woodward, "Self excited induction machine as a low cost generator," *Proceedings of IEE,* Pt. C, Vol. 131, No. 2, pp. 33-40, Mar. 1984.

[3] S. Rajakaruna and Naing Naing Maw, "Unregulated performance of an induction generator in an isolated micro hydro power plant," *Proceedings of 7th International Power Engineering Conference,* pp. 1 ~ 6, Nov. 29-Dec. 2, 2005.

[4] G. M. Demetriades, "The use of induction generators for small-scale hydroelectric schemes in remote areas," *Proceedings of Conference on Electrotechnical, MELECON 2000*, Vol. 3, pp. 1055-1058, 29-31 May 2000.

[5] J. M. Ramirez and M Emmanuel Torres, "An Electronic Load Controller for the Self-Excited Induction Generator," *IEEE Transactions on Energy Conversion,* Vol. 22, No. 2, pp. 546-548, Jun. 2007.

[6] Juan M. Ramirez and M. Emmanuel Torres, "An Electronic Load Controller for Self-Excited Induction Generators," *Proceedings of IEEE Power Engineering Conf. 2007*, pp. 1-8. Jun. 2007.

[7] B. Singh, S. S. Murthy and S. Gupta, "Analysis and design of electronic load controller for self-excited induction Generators," *IEEE Transactions on Energy Conversion,* Vol. 21, No. 1, pp. 285-293, Mar. 2006.

[8] I. Serban, C.P. Ion, C. Marinescu and M. N. Cirstea, "Electronic Load Controller for Stand-Alone Generating Units with Renewable Energy Sources," *Proceedings of IEEE Industrial Electronics Conf. 2006(IECON'06),* pp. 4309-4312, Nov. 2006.

[9] B. Singh, G. K. Kasal, and S. Gairola, "Power Quality Improvement in Conventional Electronic Load Controller for an Isolated Power Generation," *IEEE Transactions on Energy Conversion,* Vol. 23, No. 3, pp.764-773, Sept. 2008.

[10] B. Singh, G. Kasal, A. Chandra and Kamal-Al-Haddad, "Battery Based Voltage and Frequency Controller for Parallel Operated Isolated Asynchronous Generators," *Proceedings of IEEE- ISIE Conf.* 2007, pp. 883-888, Jun. 2007.

[11] B. Singh, S.S. Murthy and S. Gupta, "Transient analysis of self-excited induction Generator with electronic load controller (ELC) supplying static and dynamic loads," *IEEE Transactions on Industry Applications,* Vol. 41, No. 5, pp. 1194-1204, Sept./Oct. 2005.

[12] B. Singh, S.S. Murthy and S. Gupta, "Analysis and implementation of an electronic load controller for a self-excited induction generator," *Proceedings of IEE, Generation, Transmission and Distribution,* Vol. 151, No. 1, pp. 51-60, Jan. 2004.

[13] Wang Jun and Yu Bo, "A novel electronic load controller: theory and implementation Electrical Machines and Systems," *Proceedings of ICEM Conf. 2001*, Vol. 2, pp. 1276-1278, Aug. 2001.

[14] B. Singh, Sanjay Gairola, A. Chandra and K. Al-Haddad, "Power Quality Improvements in Isolated Twelve-Pulse AC-DC Converters Using Delta/Double Polygon Transformer," *Proceedings of IEEE PESC Conf. 2007*, pp. 2848-2853, Jun. 2007.

[15] B Singh, P Jayaprakash and D.P Kothari, "A T-Connected Transformer and Three-leg VSC Based DSTATCOM for Power Quality Improvement," *IEEE Transactions on Power Electronics,* Vol. 23, No. 6, pp. 2710-2718, Nov. 2008.

Bhim Singh (SM'99) was born in Rahamapur, India, in 1956. He received a B.E. degree in electrical engineering from the University of Roorkee, Roorkee, India, in 1977, and an M.Tech. and a Ph.D. in electrical engineering from the Indian Institute of Technology (IIT)-Delhi, New Delhi, India, in 1979 and 1983, respectively. In 1983, he joined the Department of Electrical Engineering, University of Roorkee, as a Lecturer, and in 1988, became a Reader. In December 1990, he joined the Department of Electrical Engineering, IIT-Delhi, as an Assistant Professor. He became an Associate Professor in 1994 and a Professor in 1997. He has received the Khosla Research Prize of the University of Roorkee in 1991. He is a recipient of the JC Bose and Bimal K Bose awards of The Institution of Electronics and Telecommunication Engineers (IETE) for his contribution in the field of Power Electronics in 2000. He is also a recipient of the Maharashtra State National Award of the Indian Society for Technical Education (ISTE) in recognition of his outstanding research work in the area of Power Quality in 2006. He has received the PES Delhi Chapter Outstanding Engineer Award for 2006. He has been the General Chair of the IEEE International Conference on Power Electronics, Drives and Energy Systems (PEDES'2006) held in New Delhi. His current research interests include power electronics, electrical machines and drives, active filters, flexible ac transmission systems (FACTS), high-voltage dc (HVDC) and power quality. Dr. Singh is a Fellow of the Indian National Academy of Engineering (INAE), the National Academy of Science, India (NASI), the Institution of Engineers (India) (IE (I)), and the Institution of Electronics and Telecommunication Engineers (IETE). He is a Life Member of

the Indian Society for Technical Education (ISTE), the System Society of India (SSI), and the National Institution of Quality and Reliability (NIQR). He is also a Senior Member of the Institute of Electrical and Electronics Engineers (IEEE).

V. Rajagopal was born in Kazipet, Warangal, India, in 1969. He received an AMIE (Electrical) degree from The Institution of Engineers, India, in 1999 and an M.Tech degree from the Uttar Pradesh Technical University, India, in 2004. His areas of interest include power electronics and drives, renewable energy generation and applications, FACTS, and power quality. He is currently working on a Ph D at the Department of Electrical Engineering, Indian Institute of Technology (IIT) Delhi, India. He is a life member of the Indian Society for Technical Education (ISTE) and the Institution of Engineers, India (IE (I)).